CORROSION SCIENCE AND TECHNOLOGY, Vol.18, No.5(2019), pp.155~167
[Research Paper]
pISSN: 1598-6462 / eISSN: 2288-6524
DOI: https://doi.org/10.14773/cst.2019.18.5.155

Experimental Investigation and Quantum Chemical Calculations of Some (Chlorophenyl Isoxazol-5-yl) Methanol Derivatives as Inhibitors for Corrosion of Mild Steel in 1 M HCl Solution

Rogayeh Sadeghzadeh[1], Ladan Ejlali[1], Moosa Es'haghi[1,†], Hadi Basharnavaz[2], and Kambiz Seyyedi[1]

[1]*Department of Chemistry, Tabriz Branch, Islamic Azad University, Tabriz, Iran*
[2]*Department of Chemistry, Faculty of Science, University of Mohaghegh Ardabili, P.O. Box 179, Ardabil, Iran*

(Received June 07, 2019; Revised September 14, 2019; Accepted September 16, 2019)

In this study, two novel Schiff base compounds including (3-(4-Chlorophenyl isoxazole-5-yl) methanol and (3-(2,4 dichlorophenol isoxazole-5-yl) methanol as corrosion inhibitors for mild steel in 1 M hydrochloric acid solution were investigated by potentiodynamic polarization, electrochemical impedance spectroscopy (EIS), and density functional theory (DFT) computations. The results showed that the corrosion inhibition efficiency (*IE*) is remarkably enhanced with the growing concentration of the Schiff base inhibitors. The results from Tafel polarization and EIS methods showed that *IE* decreases with gradual increments of temperature. This process can be attributed to the displacement of the adsorption/desorption balance and hence to the diminution of the level of a surface coating. Also, the adsorption of two inhibitors over mild steel followed the Langmuir adsorption isotherm. Too, the results of the scanning electron microscope (SEM) images showed that the Schiff base inhibitors form an excellent protective film over mild steel and verified the results by electrochemical techniques. Additionally, the results from the experimental and those from DFT computations are in excellent accordance.

Keywords: *Corrosion inhibitor, Mild steel surface, Hydrochloric acid solution, Electrochemical techniques, Density functional theory*

1. Introduction

Intense corrosion problems of mild steel especially in the acid medium owing to the extensive use of HCl solution cleaning, acid pickling, oil-wet cleaning, and acid descaling processes of mild steel surfaces is the common form of corrosion and directly impacts its cost and safety [1-6]. Therefore, studying suitable inhibitors in order to control the corrosion of mild steel in HCl solutions and decrease acid consumption, have attracted many investigators in recent years [7-11]. Using organic compounds as a corrosion inhibitor is a popular and frequent method for prevention and corrosion control [12-17]. The existing studies indicated that organic materials as inhibitors act through adsorption and the block of the active corrosion sites between the inhibitors and the metal surface [18-22]. The heterocyclic systems including electronegative elements (such as P, S, N, and O) and π electrons due to donating electrons for facilitating inhibitors adsorption over mild steel surface have been widely studied in acidic solutions [23-30]. Nowadays, Schiff base compounds considered as corrosion inhibitors have attracted more attention thanks to several advantages such as sensitivity, excellent selectivity, and high stability. These unique properties make Schiff base compound a promising material in different applications such as inorganic, biological, and analytical chemistry rather than that of corresponding aldehydes and amines [31-36].

Seifzadeh co-workers [37] studied the inhibition effect of the 5-CM-Salophen inhibitor on mild steel corrosion in hydrochloric acid solutions via electrochemical techniques. They found that *IE* significantly increased to 96.25% for 10 mg/L of inhibition concentration. The corrosion inhibition of some inhibitor compounds base on diphenolic, namely, 1,3-bis[2-(2-hydroxy benzylidenamino) phenoxy] propane (P1), 1,3-bis[2-(5-chloro-2-hydroxybenzyliden amino) phenoxy] propane(P2), and 1,3-bis[2-(5-bromo-2-hydroxybenzylidenamino) phenoxy] propane (P3) for mild steel in 1 M HCl solution were reported by Yurt co-workers [38] using electrochemical methods. The obtained results indicated that the *IE* of these in-

†Corresponding author: eshaghi.m@iaut.ac.ir

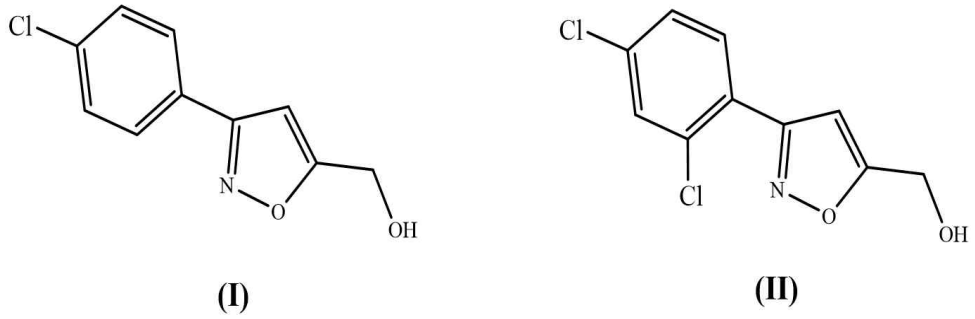

Fig. 1 Chemical structure of prepared Schiff base compounds.

hibitors obeys the order P1*(IE=85.14%)* > P3*(IE=73.5%)* > P2*(IE=68.55%)*, which is due to the substitution of chlorine and bromine elements on the aromatic ring of inhibitor compounds. In the similar work, Kumaravel *et al.* [39] studied the *IE* of the prepared unsymmetrical Schiff base compound, namely, (2Z,4E)-4-((2-(((E)-1-phenylethylidene) amino) propyl) imino) pent-2-en-2-ol using in 0.5M H_2SO_4 and 1M HCl solutions. The results revealed that Schiff base compound as an inhibitor is the best inhibitor with *IE* of approximately 92% at the presence of 600 mg/L additive concentration.

In the literature, studies concerning the inhibition of mild steel corrosion using Schiff base compounds indicated that *IE* significantly increased to addictive these compounds on a variety of substrate. Additionally, from these studies, it was known that there are no reports based on Schiff base (3-(4-Chlorophenyl isoxazole-5-yl) methanol (compound I) and (3-(2,4dichlorophenol isoxazole-5-yl) methanol (compound II) in order to introduce suitable materials for use in inhibitors for corrosion of mild steel surface.

In this work, the corrosion inhibition influence of inhibitor compound I and II on mild steel corrosion in 1M HCl solution were investigated using two various electrochemical techniques. Furthermore, the communication between the structure of Schiff base materials and the *IE* were carried out using quantum chemical computations based on density functional theory (DFT) as a powerful tool for the determination of various quantum chemical parameters including, orbital energies, band gap energy (E_g), and dipole moments [40-45].

2. Experimental

2.1. Materials

2.1.1. Preparation of Schiff base inhibitors

The optimized structures of the utilized inhibitor compounds are displayed in Fig. 1. These inhibitors were prepared via the condensation reaction of an equimolar benzaldoximesnamely: 4-chlorobenzaldoxime, 2,4-chlorobenzaldoxime and N-chlorosuccinimide, according to reference [46]. It should be noted that the anhydrous dichloromethane was used as a solvent. Their action blend was stirred at 25 °C for 1h and then, dropwise propargyl alcohol (20 mmol) followed by trimethylamine was added to the obtained liquid. The obtained product was refluxed and stirred for 6h. After that, it was cooled to 25 °C and washed with pure water and dried with sodium carbonate. The synthesis of the final Schiff base compounds was confirmed using FT-IR and ^{1}H NMR techniques.

(3-(4-Chlorophenyl isoxazole-5-yl) methanol: FT-IR (KBr,cm^{-1}): 3294 (O-H), 2928 (C-H), 1488, 1598, 1657 (C=C,C=N); ^{1}H NMR($CDCl_3$, 400MHZ, ppm): 4.78(s, 2H, CH_2), 6.51(s, 1H, isoxazole-H), 7.26-7.67(m, 4H, ArH), 8.08(bs, 1H, OH)

(3-(2,4 dichlorophenolisoxazole-5-yl) methanol: FT-IR (KBr,cm^{-1}): 3400(O-H), 3100-3120(C-H), 2960-3050 (-CH), 1450, 1530, 1550, 1600(C=C,C=N); ^{1}H NMR ($CDCl_3$, 400MHz, ppm): 2.54(bs,OH), 4.84(S, CH, CH_2), 6.71 (s, 1H, isoxazole-H),7.23-7.77(m, 3H, ArH)

2.1.2. Mild steel substrates

The investigated mild steel samples were commercial MS bars. The mild steel samples with a size of 1 cm × 1 cm × 1 cm were mounted with polyester resin (with an exposed area of 1 cm^2) utilizing MS strip as a working electrode for potentiodynamic polarization and EIS methods.

2.2. Methods

2.2. Electrochemical techniques

Potentiodynamic polarization and EIS measurements were carried out by a AUTOLAB potentiostat-galvanostat/Nova software using a conventional electrochemical cell of three electrodes, including of a working electrode (mild steel sample with 1cm^2 surface area), an Ag/AgCl

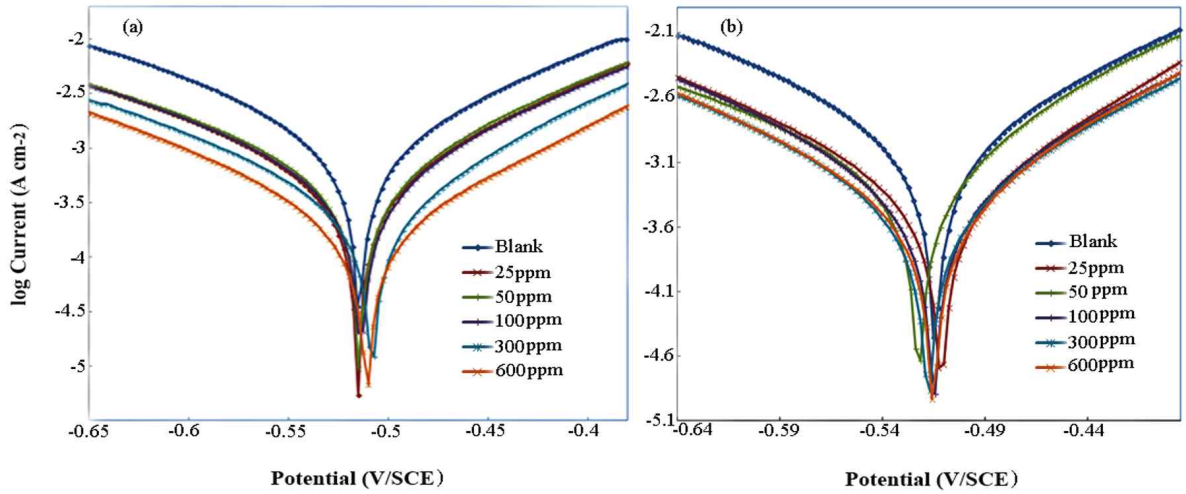

Fig. 2 Tafel polarization plots for mild steel in 1 M HCl solution in the absence (blank) and presence of different concentrations of Schiff base (a) compound I and (b) compound II at temperature of 303.3 °K.

Table 1 Corrosion parameters for the mild steel at different concentrations of the inhibitors in 1M HCl solution in temperature of 303.3°K bypotentiodynamic polarization method

concentration		R_p (Ω/cm^2)	B_a (mv/dec)	B_c (mv/dec)	I_{corr} $(\mu A/cm^2)$	$-E_{corr}$ $(V\ vs.\ Sat)$	IE%
Compound I	Blank	10.68	64.81	60.60	342.92	527.25	-
	25ppm	70.79	65.98	68.86	237.74	525.27	84.91
	50ppm	74.84	76.46	88.26	206.72	524.26	85.72
	100ppm	78.46	53.94	47.12	152.59	516.21	86.38
	300ppm	106.40	86.49	116.47	139.22	509.88	89.96
	600ppm	163.15	100.34	102.50	134.97	502.88	93.45
Compound II	25ppm	51.87	84.96	140.21	252.13	525.34	79.41
	50ppm	78.86	69.47	76.36	210.33	521.24	86.45
	100ppm	82.57	85.27	88.45	178.36	515.26	87.06
	300ppm	95.04	85.71	101.78	152.62	511.92	88.76
	600ppm	98.79	75.75	100.39	139.92	515.49	89.18

saturated calomel electrode (SCE), and a Pt sheet as counter electrode (CE) was performed for Tafel polarization and EIS measurements. Polarization data were obtained with a scan rate of 2 mVs^{-1} in the maximum overvoltage 200 mV. Impedance data were carried out in the frequency range of 1 10 MHz at the open circuit potential using exerting 10 mV sine wave AC voltage. All electrochemical tests were performed at 25 °C under environmental pressure utilizing 100 mL of corrosive solution. The impedance and Tafel polarization results were carried out for the sample sat various temperature and concentration of Schiff base inhibitors.

2.3. SEM analysis

To investigation surface morphology of the samples after 2h immersion in HCl solution without inhibitor and with 600 ppm of inhibitor, SEM images were carried out using SEM (LEO, VP 1430) model.

2.4. Density functional theory calculations

All computations were performed by the Gaussian 09 code. All geometry structures were carried out using the DFT computations at the B3LYP/6-311G**(d, p) basis

set. The important quantum parameters such as lowest unoccupied molecular orbital energy (E_{LUMO}), highest occupied molecular orbital energy (E_{HOMO}), E_g, and μ_D have been computed and discussed.

3. Results and discussion

3.1. Polarization measurement

Potentiodynamic polarization plots for mild steel in 1 M HCl solution without and with different concentrations of Schiff base compound I and II at 303.3 K temperatures are displayed in Fig. 2. The electrochemical parameters such as corrosion potential (E_{corr}), anodic and cathodic Tafel slope (β_a and β_c), corrosion current density (I_{corr}), polarization resistance (R_p), and percentage inhibition efficiency ($IE\%$) were computed by applying the extrapolation technique for the Tafel polarization plots and summarized in Table 1. It should be noted that $IE\%$ was obtained as the following relation (1):

$$(IE\%) = [1 - (\frac{I_{corr}}{I^{\circ}_{corr}})] \times 100 \quad (1)$$

where I°_{corr} and I_{corr} are the corrosion current density in the uninhibited acid and inhibited acid, respectively. The R_p was calculated from the β_a and β_c for the anodic and cathodic branches by Stern – Geary equation displayed in relation (2):

$$R_p = \frac{B_a B_c}{2.303(B_a + B_c)} \times \frac{1}{i_{corr}} \quad (2)$$

The results of Tafel polarization curves revealed that with the addition of the inhibitors, the i_{corr} for anodic and cathodic reactions was reduced and, hence, prevents the corrosion of the mild steel in 1 M hydrochloric acid solution. No considerable variation in the amounts of corrosion potential is seen except the shift in amounts to the positive direction in the attendance of the inhibitor compound compared with the blank, which may be observed to show control on the anodic and cathodic reactions and therefore they act as mixed-type inhibitor. From Table 1, it was found that the amounts of i_{corr} significantly diminish with an increment in the inhibitor concentration. It should be noted that the decrease in the values of i_{corr} is owing to the blocking of the active centers present over mild steel surface. Based on the obtained results, it can be concluded that the IE remarkably increases with an enhancement in the Schiff base compound concentration.

3.2. EIS

The Nyquist curves for mild steel in 1M hydrochloric acid solution absence (blank) and the presence of different concentrations of the Schiff base material I and II at 303.3 K temperatures are displayed in Fig. 3. From this figure, it can be seen that the Nyquist plot of mild steel in the absence and presence of several concentrations of the Schiff base compounds a little depressed semicircular shape, which indicates that corrosion of mild steel in 1 M HCl solution is essentially controlled using an electron transfer process. Furthermore, the Nyquist curves are identified using one capacitive loop and also the diameter of the loop enhances with growing inhibitor concentration, which is in excellent accordance with the other report [49].

The deflection from the ideal format which is shown as a depressed semicircle at the center under the real axis is given to the frequency scattering of impedance owing

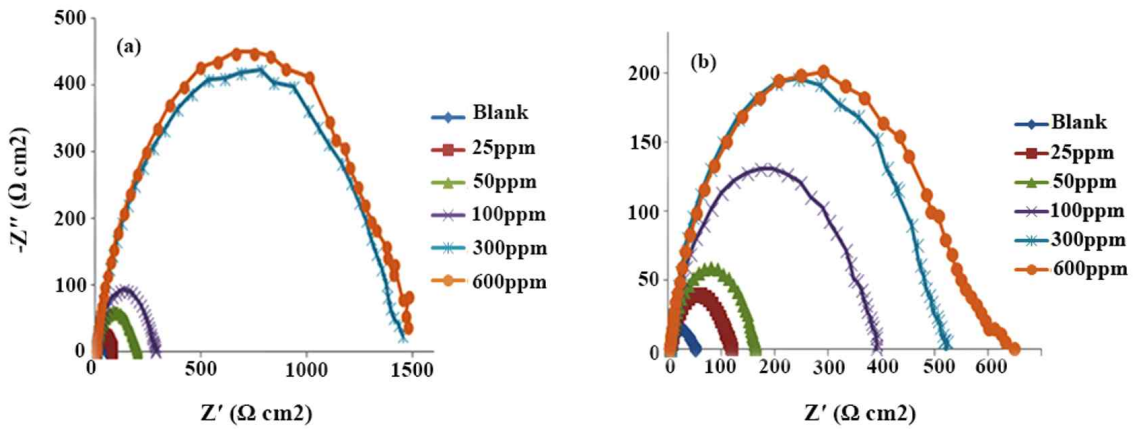

Fig. 3 Nyquist plots of EIS measurements of the mild steel in uninhibited 1 M HCl solution and with various concentrations of Schiff base (a) compound Iand (b) compound II at temperature of 303.3°K.

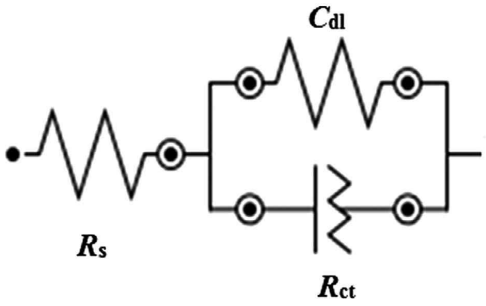

Fig. 4 The proposed equivalent circuit model for the investigated system.

to the lack of smoothness of the mild steel and adsorption of the different inhibitors [50]. As a result, pure double-layer capacitors can be described very well in such circumstances using a transfer function with constant phase elements (CPE) and the impedance is demonstrated by relation (3):

$$Z_{CPE} = Y_{\circ}^{-1} (j\omega)^{-n} \quad (3)$$

In equation Y_o is a constant with dimensions of (in $\Omega^{-1}S^{n}cm^{-2}$), ω is the angular frequency given in radians per second, j is the fictitious number and is equal to the square root of -1, and the coefficient n represents the deviated degree of the capacitance of the double layer from ideal and ranges from 0 to 1, For n = 1 a capacitance withC = Q and for n = -1 an inductance with = Q^{-1}, for n = 0, Z_{CPE} illustrates a resistance withR = Q^{-1}.

The Nyquist curve was fitted using a simple Randle's equivalent circuit, presented in Fig 4, including the solution resistance (R_s), double layer capacitance (C_{dl}), and the charge transfer resistance (R_{ct}). The double-layer capacitance can be computed from the amounts of Y_o and n by the following relation (4) [51].

$$C_{dl} = (Y_{\circ}\omega^{n-1}) \sin[n(\pi/2)]^{-1} \quad (4)$$

A decline can be observed in the magnitude of C_{dl} with growing the concentration of inhibitor compounds, which indicates increasing the thickness of electric double-layer with the creation of an inhibitor layer over mild steel surface in hydrochloric acid solution. The inhibition efficiency gained by the EIS measurements was computed by the following relation in which *Rct* and Rct° are the charge transfer resistances in uninhibited and inhibited solution, respectively.

$$IE\% = \left[\left(1 - \frac{Rct}{R_{ct}^{\circ}}\right)\right] \times 100 \quad (5)$$

It should be noted that the Nyquist plots were fitted using a simple Randle's equivalent circuit and the obtained results are summarized in Table 2. As can be observed in this Table, the R_p and $CPE_{(dl)}$ amount increase and decrease as the concentration of inhibitors enhance, respectively. Enhance in the diameter of the capacitive loop manifests the formation of a protective layer on the mild steel surface, which provides higher resistance versus electron transfer reactions happening at the metal-electrolyte interface zone. Besides, diminish in $CPE_{(dl)}$ with the increasing concentration of inhibitor can be attributed to adsorption of inhibitors over the mild metal surface by substituting pre-adsorbed H_2O molecules, lower electrical

Table 2 Impedance parameters for the corrosion of mild steel in 1 M HClsolution in the absence and presence of different concentrations of compound I and II at temperature of 303.3 °K

concentration		R_s (Ω/cm^2)	$CPE_{(dl)}$(μF/cm^2)	*n*	R_p (Ω/cm^2)	*IE%*
Compound Ⅰ	Blank	2.79	130.0	0.87	41.7	-
	25ppm	3.08	84.1	0.86	70.8	39.78
	50ppm	3.24	78.3	0.82	173.0	74.75
	100ppm	3.18	73.0	0.82	253.5	82.66
	300ppm	3.64	44.2	0.80	1490.0	97.02
	600ppm	3.31	38.5	0.81	1506.0	97.05
Compound Ⅱ	25ppm	2.78	78.9	0.85	103.4	58.09
	50ppm	3.58	66.5	0.86	156.7	72.24
	100ppm	3.55	63.2	0.87	401.4	89.01
	300ppm	3.28	61.0	0.86	528.8	91.63
	600ppm	3.82	56.0	0.84	608.3	92.73

Table 3 Activation energy (E_a) of two Schiff base compounds

concentration		E_a (kj/mol)
Compound I	Blank	34.09
	25ppm	39.91
	50ppm	41.94
	100ppm	41.97
	300ppm	42.18
	600ppm	42.62
Compound II	25ppm	34.53
	50ppm	34.74
	100ppm	35.07
	300ppm	35.17
	600ppm	41.59

permittivity of adsorbed inhibitors compared to H_2O molecules, as well as the enhanced thickness of the protective layer. Based on the impedance data results, it is clear that the *IE* considerably enhance with the growing inhibitor concentrations, which shows the increase of surface resistance by the inhibitor compounds and the growing inhibition of mild steel corrosion. It should be noted that the values obtained for inhibition efficiency from different teachings including potentiodynamic polarization and impedance are in excellent agreement.

3.3. Effect of temperature

In order to investigate the effect of temperature over corrosion of mild steel and its inhibition, we computed Tafel polarization and EIS experiments in the without and with of Schiff base compounds in the temperature range of 303.3 – 343.3 K and the results of these calculations demonstrated that by growing the temperature from 303.3 to 343.3 K, the *IE%* for 600 ppm of compound I decreases from 93.45 to 76.14% and from 97.05 to 80.31% in Tafel polarization and EIS experiments, respectively. The diminution in the *IE%* with enhance in the temperatures is owing to the shift of the adsorption/desorption balance towards the inhibitor's desorption and in this way the diminution of the degree of surface coverage. The *IE* computed from the EIS method, indicate a similar trend as those obtained from the potentiodynamic polarization method [47,48]. Furthermore, from Nyquist curves in the temperature range of 303.3 – 343.3 K, it was found that the size of the semicircles diminished with increasing of temperature. This process is an indicator of rising corrosion rate of the samples with temperature in the blank and inhibitor-containing corrosive solutions.

Furthermore, it should be noted that the activation energy *(E_a)* performs a key role in understanding the mechanism of action of Schiff base inhibitors. In order to calculate the E_a of the corrosion process in the presence and absence of Schiff base inhibitors, using Arrhenius equation (6):

$$i_{corr} = Aexp(\frac{-E_a}{RT}) \quad (6)$$

where E_a representing the activation energy of the corrosion process, is the gas constant, absolute temperature, the Arrhenius constant and the corrosion current density. The E_a amounts can be determined from the slopes of Arrhenius plots (logi_{corr} vs. 1/T). Therefore, the value of E_a could be obtained by calculating the linear slope ($\frac{-Ea}{R}$) of equation (6) (see Fig. 5) and are summarized in Table 3. The calculated values for linear regression coefficients are close to unity, indicating that the corrosion of mild

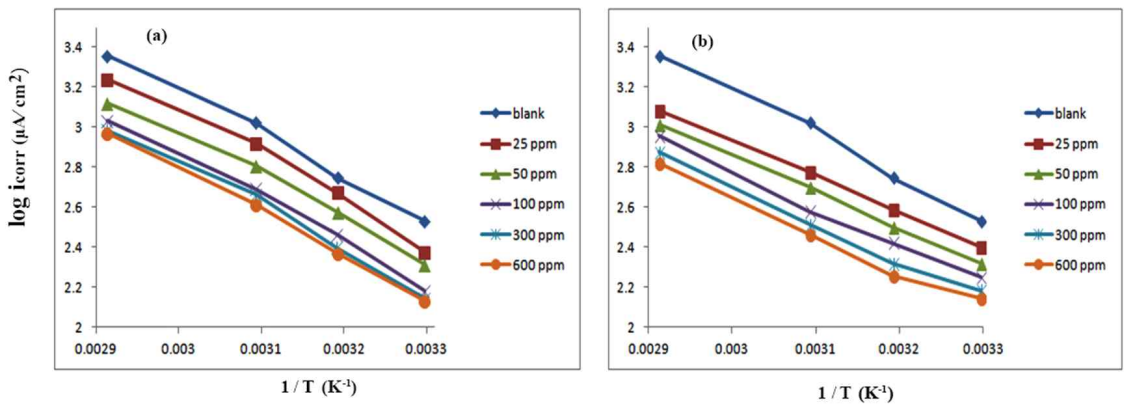

Fig. 5 Arrhenius slopes calculated from corrosion current density for mild steel at different concentration of inhibitors in:(a) compoundI and (b) compound II.

Table 4 Thermodynamic parameters for adsorption of compound Ⅰ and Ⅱ on mild steel in 1 M HCl solution at different temperatures from the Langmuir adsorption isotherm

	Temperature(°K)	Intercept	Slope	K_{ads}	$\triangle G°_{ads}$(kj/mol)	R^2
Compound Ⅰ	303.3	0.00407	1.2324	245.700	-23.983	0.993
	313.3	0.00401	1.2352	249.376	-24.817	0.991
	323.3	0.00146	1.4022	684.462	-28.318	0.992
	343.3	0.00134	2.0470	746.268	-29.437	0.941
Compound Ⅱ	303.3	0.00207	1.5424	483.091	-25.689	0.999
	313.3	0.00156	1.9290	641.025	-27.274	0.993
	323.3	0.00045	2.1724	2222.22	-31.485	0.993
	343.3	0.00036	3.9698	777.77	-33.072	0.986

steel in HCl solution can be explained using the kinetic model. The E_a values in the presence of Schiff base inhibitors are higher than that of the blank HCl solution. Enhancement in the E_a amounts along with higher inhibition efficiencies with growing inhibitor concentration can be attributed to the strong adsorption of Schiff base inhibitors.

3.4. Adsorption isotherms

In an attempt to investigate the thermodynamics included during adsorption of inhibitors on mild steel surface in 1 M HCl solution, we have fitted the experiential data points through several adsorption isotherms involving the Frumkin, Temkin, Langmuir, and Freundlich isotherms. The most suitable isotherm was chosen among isotherm models, with using regression coefficient R^2 (see Table 4).

As a result, the most suitable model was Langmuir isotherm which was fit with experiential data, with all linear R^2 very near oneness. In other words, it proves that the adsorption process of compound I and II on the mild steel in 1M hydrochloric acid solution is according to Langmuir isotherm containing physical and chemical adsorption.

$$\frac{C_{inh}}{\theta} = \frac{1}{K_{ads}} + C_{inh} \quad (7)$$

$$K_{ads} = \frac{1}{55.5} exp(\frac{-\Delta G^{\circ}_{ads}}{RT}) \quad (8)$$

where K_{ads} is the balance constant for the adsorption-desorption process and C_{inh} is the inhibitor concentration, Θ is the surface coverage owing to inhibitor adsorption, and $\triangle G°_{ads}$ is the standard free energy of the adsorption equations. From equation 7, a plot of (C/Θ) versus C produced direct lines with intercept log K_{ads} (see Fig. 6). The results of this figure indicated that adsorption of inhibitor compound Ⅰ and Ⅱ on mild steel surface at 303.3 K obey Langmuir adsorption isotherm. It should be noted that adsorption of Schiff base inhibitors in all of the temperature obeyed Langmuir adsorption isotherm.

The results of a literature review indicated that the if the value of $\triangle G°_{ads}$ is about -20 kJ/mol, the inhibitors adsorption process on the metal surface is physisorption, which includes electrostatic interactions between the Schiff base compounds and the surface of metals, while its amount of -40 kJ/mol or more is determined as chemisorption owing to electron transfer between the adsorbent surface and adsorbate. In this investigation, the amounts of $\triangle G°_{ads}$ for the compound I and compound II at 303.3 K, vary from -23.983 and -25.689 kJ mol^{-1}, respectively, offering both chemisorption and physisorption mechanism (including mixed mode). It should be noted that the adsorption of Schiff base compounds at all of the temperatures on the mild steel surface involves both chemicals as well as physical interactions. In chemisorption mechanism, the electron transfer between π-electrons of Schiff base compounds and d-orbitals of mild steel are forming coordination bonds**.** Furthermore, physisorption mechanism owing to electrostatic interaction between Schiff base compounds and mild steel surface.

3.5. SEM

The SEM images for polished and corroded mild steel

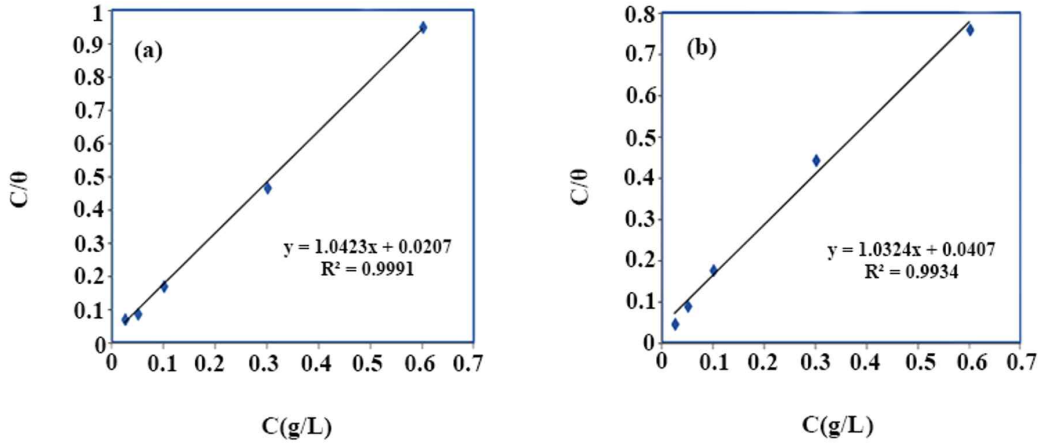

Fig. 6 Langmuir isotherm for adsorption of Schiff base (a) compoundI and (b) compound IIat 303.3 °K on the mild steel surface.

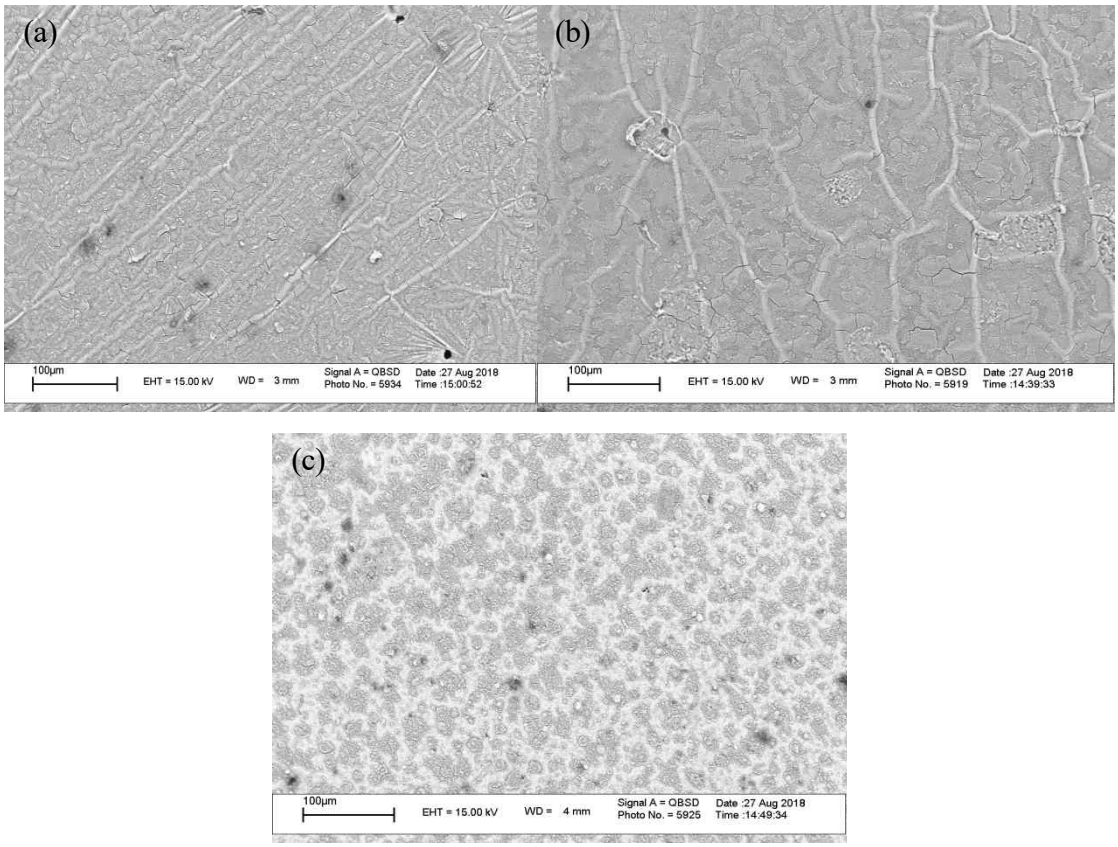

Fig. 7 SEM micrographs of the surface of the mild steel after 2 hours of immersion in 1 M HCl solution (a) blank HCl, (b) compound I, and (c) compound II.

in 1 M hydrochloric acid solution without (blank) and with of 600 ppm concentrations of Schiff base compound I and II at 303.3 K after 2h of immersion are illustrated in Fig. 7a-c. From this figure, it can be observed that the blank sample surface is very rough, cracks and pits can be seen at the surface thanks to severe corrosion, whereas the surface of the samples with 600 ppm of Schiff base compounds are smooth because of formation of protective inhibitor film which decreases corrosion of these samples.

3.6. Quantum chemical study

DFT calculations were performed to release donor – acceptor interactions between the Schiff base compounds and metallic surface. The optimized structure and adsorption energy (E_{ads}) of Schiff base compound I and II are represented in Table 5a and b. The E_{ads} for adsorption of Schiff base compounds over the mild steel surface were computed from the following equation:

$$E_{ads} = E_{MS\ surface-Schiff\ base} - E_{MS\ surface} - E_{Schiff\ base} \quad (9)$$

where $E_{MS\ surface-Schiff\ base}$, $E_{Schiff\ base}$, and $E_{MS\ surface}$ are the total energy of Schiff base compounds adsorbed on mild steel surface, Schiff base compounds, and mild steel surface, respectively. Therefore, a negative adsorption energy value reveals the adsorption is energetically favorable, while a positive E_{ads} value shows an unstable system. From these tables, it can be observed that the E_{ads} of inhibitor compound I and II on the mild steel surface are -1.93 and -1.82 eV, respectively. According to the obtained results, the adsorption of Schiff base inhibitors on position 2 of the mild steel surface is higher than that of other positions. This process can be attributed to the covalent bond between mild steel surface and electron pairs of N atom in Schiff base compounds (see Fig. 8a

Table 5a Optimised geometrical configurations all positions of compound I with corresponding energies

Position	Structure	Eads(Hartree)	Eads(eV)
pure	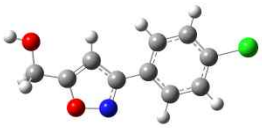	-1051.023739	-
1	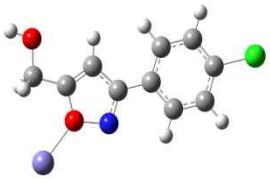	-2314.409346	-0.225
2	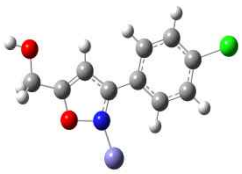	-2314.47237	-1.93
3	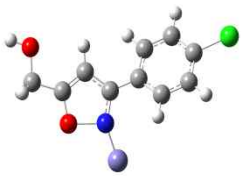	-2314.465400	-1.74
4	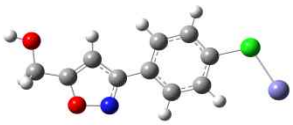	-2314.407010	-1.90
5		-2314.423442	-0.598

Table 5b Optimised geometrical configurations all positions of compound II with corresponding energies

Position	Structure	E_{ads}(Hartree)	E_{ads}(eV)
pure	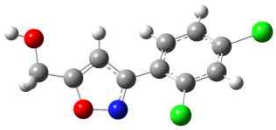	-1510.587164	-
1	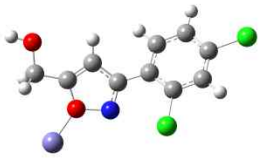	-2773.993522	-0.789
2	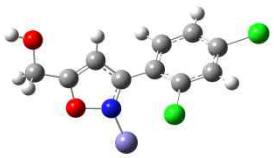	-2774.031618	-1.82
4	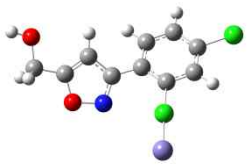	-2773.903359	-1.66
5	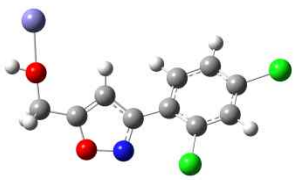	-2773.919597	-1.19
6	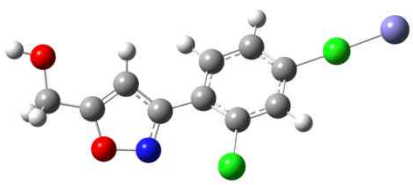	-2773.970250	-0.157

and 8b). Based on these results, it can be concluded that the interaction between mild steel surface and Schiff base compound I is stronger than that of compound II, which is in good accordance with the experimental results.

Results for calculated parameters such as E_{LUMO}, E_{HUMO}, $E_g = E_{LUMO} - E_{HUMO}$ (band gap energy), μ_D are presented in Table 6. It should be noted that a high E_{HUMO} indicates intrinsic electron-donating tendency to an electron acceptor, while a high E_{LUMO} shows intrinsic electron receiving tendency of a molecule. On the other hand, fewer values of the band gap energy will cause an excellent *IE*, as the energy in order to remove a charge from the HOMO will be very low. Additionally, the results of DFT calculations indicated that the band gap energy of Schiff base compound I and II obey the order: compound II > compound I. From the above discussion, it can be deduced that the compound I has lower band gap energy value compared to compound II, which confirms that the *IE* of compound I is greater than that of compound II.

Table 6 Quantum chemical parameters of used Schiff bases obtained from B3LYP/6-311G (d, p) method**

Compound	$E_{HOMO}(eV)$	$E_{LUMO}(eV)$	$E_g(eV)$	E	μ_D (Debye)	(eV)
(I)	-0.12005	-0.08388	0.036	-2314.47237	4.90	-1.93
(II)	-0.15645	-0.69230	0.087	-2774.03161	-8.13	-1.82

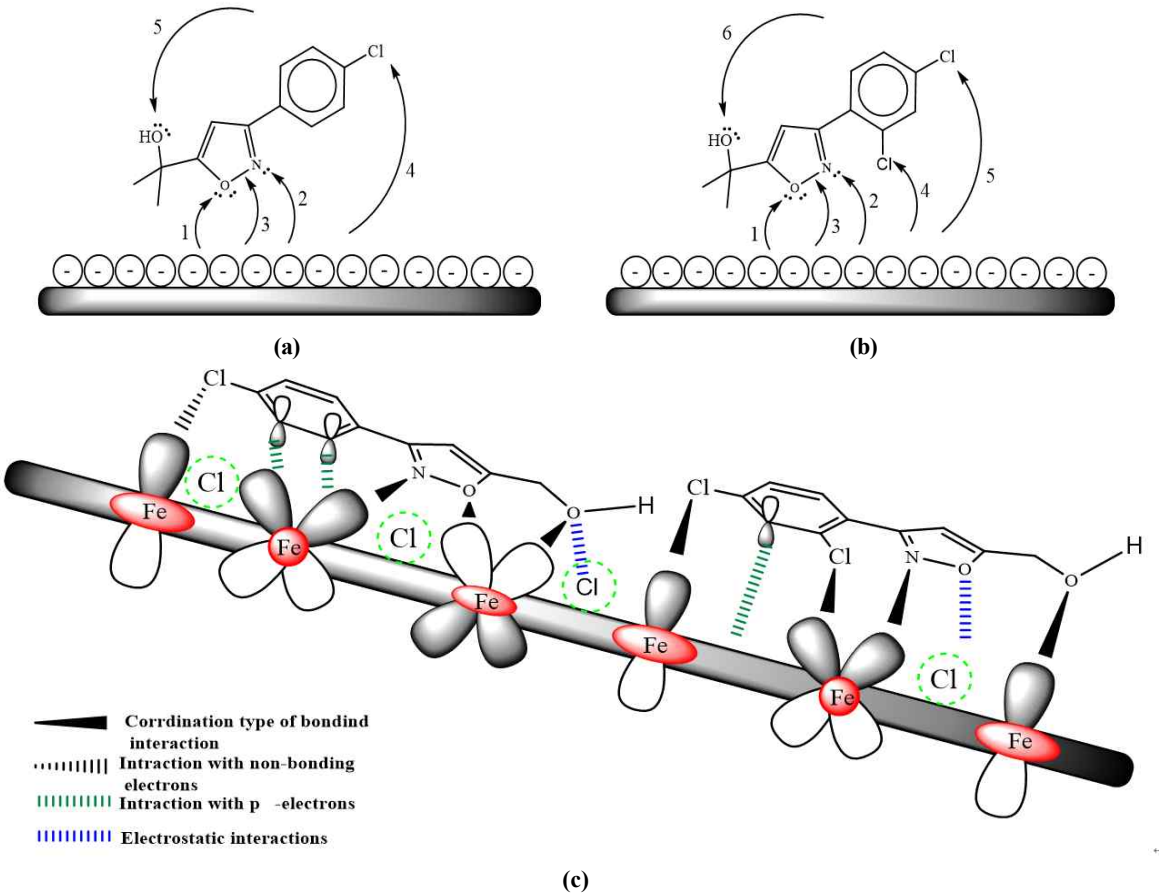

Fig. 8 Schematic graphical illustration of different types of interactions proposed for the adsorption of Schiff base inhibitors on mild steel in 1M HCl solution.

4. Mechanism of inhibition

The inhibitory action in most cases is by the adsorption of inhibitors over the mild metal surface. The adsorption process is related to the chemical behavior such as structure and presence of donor atoms in the inhibitor molecule (such as S, N, and O elements). The adsorption of inhibitor molecules over the metal surface can be done by several modes including chemisorption and physisorption. The adsorption process depends on various important factors such as molecular size, the number of active sites, geometry, the electron of surface, the type of interaction between inhibitors and metal surface, distributed electronic charge of inhibitor molecules as well as kind of electrolyte. According to these parameters, it can be deduced that the inhibitors were adsorbed over mild steel surface in HCl solution through physically and chemically mechanism. According to gravimetric and electrochemical results and surface analysis, the graphical design of various adsorption positions of inhibitors over mild steel interface is represented in Fig. 8c. There could be different possible mechanisms for the adsorption of Schiff base inhibitors on mild steel surface namely: 1) electrostatic interactions between the protonated Schiff base compounds and the pre-adsorbed Cl^- ions; 2) interaction between unshared valence electron pairs of heteroatoms (N and O) and vacant

d-orbital of Fe atoms, or donor-acceptor interactions between the vacant d-orbital of Fe atoms and π-electrons of aromatic ring. Therefore, Cl^- ions from the HCl solution would probably absorb over positively charged surface of the mild steel and change the electron on the mild steel from positive to negative; this process is followed by adsorption of cationic inhibitor on the negatively charged mild steel surface through electrostatic interaction and therefore supporting the physical adsorption mechanism. Besides the physical adsorption mechanism, Schiff base compounds could be chemically adsorbed over mild steel surface through creating a coordinate bond in between the electrons of hetero-atoms and vacant d-orbitals of Fe atoms.

5. Conclusions

In the present work, two novel Schiff base compounds including (3-(4-Chlorophenyl isoxazole-5-yl) methanol and (3-(2,4 dichlorophenol isoxazole-5-yl) methanol as a corrosion inhibitors for mild steel in 1M hydrochloric acid solution were investigated by potentiodynamic polarization, electrochemical impedance spectroscopy (EIS), and density functional theory (DFT) computations. The obtained results displayed that the corrosion inhibition efficiency (*IE*) remarkably enhances with the growing concentration of the inhibitors. On the other hand, the results revealed that the *IE* remarkably increased to 97.05% for 600 ppm of Schiff base (3-(4-Chlorophenyl isoxazole-5-yl) methanol concentration. Hence, this Schiff base compound is as a corrosion inhibitor for mild steel in HCl solution, in comparison with that of the other compounds. The results from Tafel polarization and EIS methods showed that *IE* decreases with gradual increments of temperature. This process can be attributed to the displacement of the adsorption/desorption balance and hence to the diminution of the level of the surface coating. Furthermore, the adsorption of two inhibitors over mild steel followed the Langmuir adsorption isotherm. Furthermore, the results of SEM images displayed that the Schiff base inhibitors form an excellent protective film over mild steel and verified the obtained result by electrochemical techniques. Additionally, the results obtained from experimental and those from DFT computations are in excellent accordance. Conclusively, we should noted that the practical and economic view point, an extensive and in-depth research is required to shift these achievements of laboratory investigations to an industrial scale.

Acknowledgment

We gratefully acknowledge financial support from the Research Council of Tabriz Branch of Islamic Azad University.

References

1. N. Eddy and E. E. Ebenso, *Pigment & Resin Technology,* **39**, 77 (2010).
2. D. S. Chauhan, K. R. Ansari, A. A Sorour, M. A Quraishi, H. Lgaz, and R. Salghi, *International Journal of Biological Macromolecules,* **107**, 1747 (2018).
3. Q. B. Zhang and Y. X. Hua, *Electrochim. Acta,* **54**, 1881 (2009).
4. M. Lagrenee, B. Mernari, M. Bouanis. M. Traisnel, and F. Bentiss, *Corros. Sci.,* **44**, 573 (2002).
5. P. P. Kumari, P. Shetty, and S. A. Rao, *Arab. J. Chem.,* **10**, 653 (2017).
6. I. Ahamad and M. A. Quraishi, *Corros. Sci.,* **51**, 2006 (2009).
7. B. E. Rani and B. B. Basu, *Int. J. Corros.,* **12**, 1 (2012).
8. C. Verma, M. A. Quraishi, and A. Singh, *J. Taibah Univ. Sci.*, **10**, 718 (2016).
9. D. Daoud, T. Douadi, H. Hamani, S. Chafaa, and M. Al-Noaimi, *Corros. Sci.*, **94**, 21 (2015).
10. K. R. Ansari, D. K. Yadav, E. E. Ebenso, and M. A. Quraishi, *Int. J. Electrochem. Sci.,* **7**, 4780 (2012).
11. H. B. Fan, C. Y. Fu, H. L.Wang, X. P. Guo, and J. S. Zheng, *Brit. Corros. J.,* **37**, 122 (2002).
12. S. Safak, B. Duran, A. Yurt, and G. Turkoglu, *Corros. Sci.*, **54**, 251 (2012).
13. A. Fiala, A. Chibani, A. Darchen, A. Boulkamh, and K. Djebbar, *Appl. Surf. Sci.*, **253**, 9347 (2007).
14. I. B. Obot, N. O. Obi-Egbedi, and N. W. Odozi, *Corros. Sci.*, **52**, 923 (2010).
15. A. Pandey, B. Singh, C. Verma, and E. E. Ebenso, *RSC Advances*, **7**, 47148 (2017).
16. A. Chetouani, B. Hammouti, T. Benhadda, and M. Daoudi, *Appl. Surf. Sci.*, **249**, 375 (2005).
17. S. A. El-Maksoud, *Electrochim. Acta,* **49**, 4205 (2004).
18. D. Ben Hmamou, M. R. Aouad, R. Salghi, A. Zarrouk, M. Assouag, O. Benali, M. Messali, H. Zarrok, and B. Hammouti, *J. Chem. Pharmaceut. Res.*, **4**, 3489 (2012).
19. L. Larabi, O. Benali, and Y. Harek, *Mater. Lett.*, **61**, 3287 (2007).
20. A. Y. Musa, A. A. Kadhum, A. B. Mohamad, and M. S. Takriff, *Corros. Sci.,* **52**, 3331 (2010).
21. O. Benali, L. Larabi, S. M. Mekelleche, and Y. Harek, *J. Mater. Sci.*, **41**, 7064 (2006).
22. H. Zarrok, A. Zarrouk, R. Salghi, M. Assouag, B. Hammouti, H. Oudda, S. Boukhris, S. S. Al Deyab, and I. Warad, *Der Pharmacia Letter,* **5**, 43 (2013).
23. K. C. Emregul, E. Duzgun, and O. Atako, *Corros. Sci.*, **48**, 3243 (2006).
24. H. Ju, Z. P. Kai, and Y. Li, *Corros. Sci.,* **50**, 865 (2008).
25. K. C. Emregul, R. Kurtaran, and O. Atakol, *Corros. Sci.,*

45, 2803 (2003).
26. K. F. Khaled, K. Babi, and N. Hackerman, *J. Appl. Electrochem.,* **34**, 697 (2004).
27. G. Bereket, C. Ogretir, and A. Yurt, *J. Mol. Struct. Theochem.,* **571**, 139 (2001).
28. S. A. El-Rehim, M. A. Ibrahim, and K. F. Khaled, *J. Appl. Electrochem.*, **29**, 593 (1999).
29. L. M. Rodriguez-Valdez, W. Villamisar, M. Casales, J. G. Gonzalez-Rodriguez, A. Martinez-Villafane, L. Martinez, and D. Glossman-Mitnik, *Corros. Sci.*, **48**, 4053 (2006).
30. F. Bentiss, M. Bouanis, B. Mernari, M. Traisnel, H. Vezin, and M. Lagrenee, *Appl. Surf. Sci.,* **253**, 3696 (2007).
31. M. A. Ashraf, K. Mahmood, A. Wajid, M. J. Maah, and I. Yusoff, *Int. Conf. Chem. Chem. Proc.*, **10**, 1 (2011).
32. A. Paul, K. J. Thomas, V. P. Raphael, and K. S. Shaju, *ISRN Corrosion*, 2012, Article ID 425878 (2012).
33. H. Ashassi-Sorkhabi, B. Shaabani, and D. Seifzadeh, *Appl. Surf. Sci.,* **239**, 154 (2005).
34. M. Hosseini, S. F. Mertens, M. Ghorbani, and M. R. Arshadi, *Mater. Chem. Phys.*, **78**, 800 (2003).
35. K. C. Emregul and O. Atakol, *Mater. Chem. Phys.,* **83**, 373 (2004).
36. G. Ceyhan, M. Tumer, M. Kose, V. McKee, and S. Akar, *J. Lumin.*, **132**, 2917 (2012).
37. D. Seifzadeh, V. Valizadeh-Pashabeigh, and A. Bezaatpour, *Chem. Eng. Commun.*, **203**, 1279 (2016).
38. A. Yurt, B. Duran, and H. Dal, *Arab. J. Chem.*, **7**, 732 (2014).
39. K. Mallaiya, R. Subramaniam, S. S. Srikandan, S. Gowri, N. Rajasekaran, and A. Selvaraj, *Electrochim. Acta,* **56**, 3857 (2011).
40. G. Gece, *Corros. Sci.*, **50**, 2981 (2008).
41. M. A. Quraishi and R. Sardar, *Mater. chem. phys.*, **78**, 425 (2003).
42. L. Tang, X. Li, L. Li, G. Mu, and G. Liu. *Surf. Coat. Technol.,* **201**, 384 (2006).
43. H. Hamani, T. Douadi, D. Daoud, M. Al-Noaimi, R. A. Rikkouh, and S. Chafaa, *J. Electroanal. Chem.*, **801**, 425 38 (2017).
44. R. G. Parr, D. P. Craig, and I. G. Ross, *J. Chem. Phys.,* **18**, 1561 (1950).
45. M. Messali, M. Larouj, H. Lgaz, N. Rezki, F. F. Al-Blewi, M. R. Aouad, A. Chaouiki, R. Salghi, and I. M. Chung, *J. Mol. Struct.*, **1168**, 39 (2018).
46. L. D. Tang, D.T. Zhang, F. G. Sun, G. Y. Duan, and J. W. Wang, *Acta Crystallogr. E*, **62**, 1298 (2006).
47. M. S. Morad and A. K. El-Dean, *Corros. Sci.*, **48**, 3398 (2006).
48. S. Zehra, M. Mobin, J. Aslam, and M. Parveen, *J. Adhesion Sci. Technol.,* **32**, 317 (2018).
49. A. Popova, *Corros. Sci.*, **49**, 2144 (2007).
50. D. K. Yadav, B. Maiti, and M. A. Quraishi, *Corros. Sci.*, **52**, 3586 (2010).
51. S. E. Manahan, *Enbironmental chemistry*, *10th ed.*, pp. 1 - 752, Taylor & Francis, OX (2017).